

LASER SURFACE CLADDING

W. M. STEEN

Metallurgy and Materials Science Department, Imperial College,
London SW7 2BP, UK

Key Words: cladding, powder feed, steel reflectance

1. DESCRIPTION OF THE PROCESS

The objective in laser cladding is to fuse an alloy on to the surface of a substrate with a minimum of dilution from the substrate. Areas are clad by overlapping single-clad tracks.

The process can be performed by either preplacing a powder on the substrate or blowing the powder into the laser-generated melt pool. It can also be done by applying the clad material as a wire sheet or plasma spraycoat or electroplate coat.

In preplaced powder cladding described by Powell (1), the laser sends a melt wave through the powder bed. Since the powder bed has a low thermal conductivity, the pool is almost thermally insulated until it reaches the substrate surface. At that moment it will freeze back, forming only a solid/liquid bond which is relatively weak compared to a full fusion bond. Continued heating will remelt the resolidified material and then cause a fusion bond to form. However, it will be seen that this allows a relatively small operating region in which there is a fusion bond with low dilution. The process is illustrated in Fig. 1. One of the principal problems with this process is the difficulty in keeping the powder in place while it is melted by the beam.

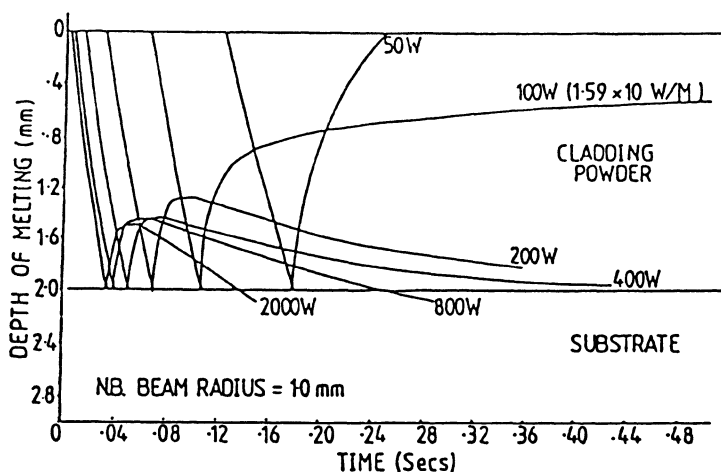


FIGURE 1. Movement of molten front with time at different laser powers.

In blown powder cladding (2,3) the powder is blown by an inert gas stream into the laser-generated melt pool, as illustrated in Figs. 2 and 3. The leading edge of the melt pool will incorporate the substrate.

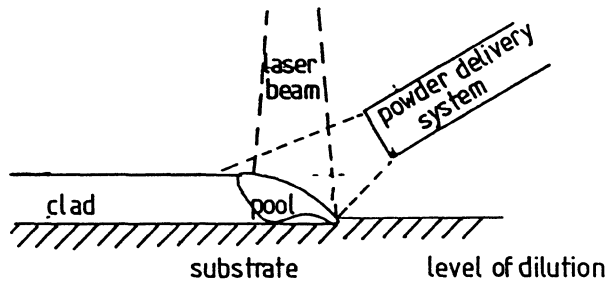


FIGURE 2. Laser cladding with blown powder.

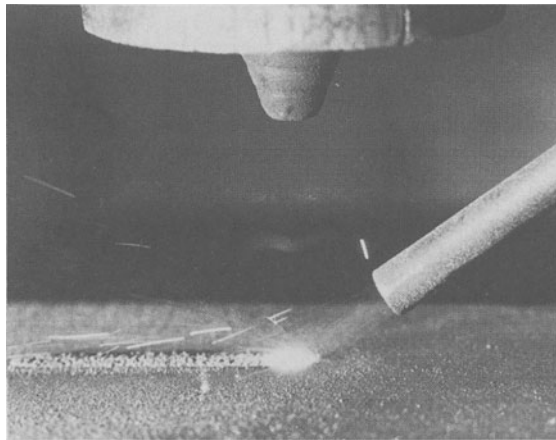


FIGURE 3. Laser cladding by powder injection.

Particles arriving in this area will be solid. If the leading edge of the substrate is also solid, then the particle will not stick and cladding will not occur. If, however, the leading edge is molten, then the particles will stick and will melt almost instantly under the power from the beam, thus forming a fusion bond. The level of dilution is controlled by the powder feed rate determining the size of the substrate's molten leading edge. Uniform clad layers are formed by overlapping single tracks, as illustrated in Fig. 4(a,b). The process critically depends upon a uniform powder feed rate. Such a feeder was developed. Its performance is illustrated in Fig. 5.



FIGURE 4. (a) Development of a uniform clad layer by overlapping.

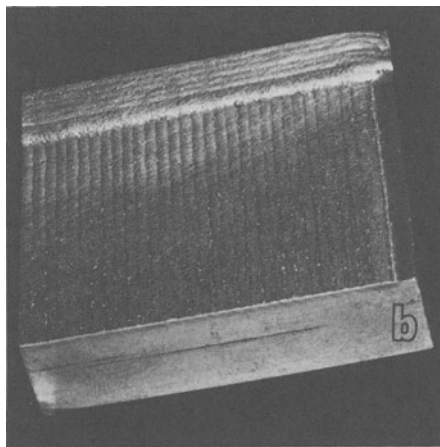


FIGURE 4. (b) a laser-clad plate. Plate thickness 12.5 mm. Single layer is 0.3 mm thick, double layer 1.5 mm thick.

If the clad material is fed as either wire or sheet, there is a problem with reflectivity and so the process is less efficient but still possible.

Consolidation of surfaces by laser remelting of plasma spray-coated or electroplated surfaces is also practiced (4,5).

The main characteristics of the blown powder process are:

- Controlled levels of dilution
- Localized heating which reduces thermal distortion and the size of the heat affected zone (HAZ)
- Controlled shape of clad within certain limits
- Smooth surface finish ($\approx 25 \mu\text{m}$)
- Good fusion bonding
- Fine quench microstructures
- Non-contact method of application
- Easily automated
- Omnidirectional
- Near isotropic mechanical properties
- Thin clad layers are possible ($>0.3 \text{ mm}$)
- Minimum surface preparation is required for many applications
- Process is flexible

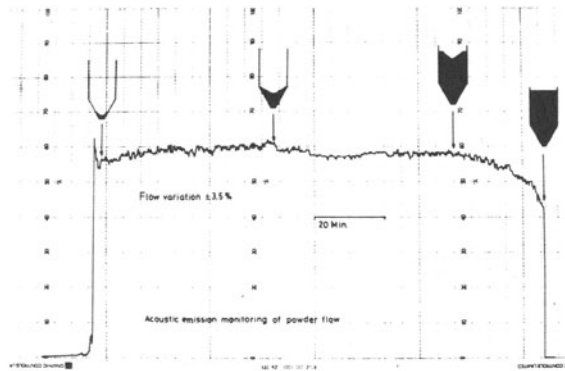


FIGURE 5. In-process monitoring of powder feed rate using an acoustic emission technique (11).

1.2. Process variations

Mixed powder feed (6): By this method alloys can be formed in situ or non-homogeneous deposits formed.

Optical feedback systems (2,3) have been developed which increase the efficiency of utilization of the beam power by around 40%.

Vibro laser cladding (7): By this method the substrate is vibrated ultrasonically while cladding proceeds. There is considerably less cracking and porosity observed.

1.3. Applications

The first industrial use of lasers in cladding was done by Rolls Royce (8) in 1981. They clad turbine blade shroud interlocks on the RG 211 engine.

Since then many companies have applied or are considering applying this process.

Eboo (9) lists the activity reported in Table 1.

1.4. Comparison with alternative processes

One reason for the great industrial interest in this process is that it is one of the very few surfacing processes which cause little thermal damage to the substrate, and relatively slight distortion (10). It is also the only fusion-cladding process which allows a patterned clad to be laid down.

Alternative processes are listed in Table 2.

2. PROCESS MECHANICS OF THE BLOWN-POWDER PROCESS

2.1. Characteristic process phenomena

The powder injection technique is fundamentally more flexible and superior to the pre-placed powder technique (11) in that localized areas of components of complex geometry can be clad with better control on dilution and clad thickness.

The use of the cladding material in the form of a powder has an added attraction due to the increased efficiency obtained in coupling the laser energy. Powder particles in or near the surface appear to enhance the absorption of laser energy. A molten pool is generated on the ground

surface when powder is injected whereas no melting is observed without powder. Metallurgically, the use of powder may reduce macro-segregation effects during solidification.

TABLE 1. Representative laser cladding efforts.

Company	Component	Comment
<u>Production Stage</u>		
Rolls Royce	Turbine blade shroud interlock	Cobalt base alloy powder feed
Pratt & Whitney	Turbine blade	PWA 694/nimonic preplaced chips
G.E.	Proprietary	Reverse machining with Ti powder feed
<u>Pilot Demonstration Stage</u>		
Combustion Eng.	Offshore drilling & production parts	Stellites, colmonoys and other alloys including carbides
	Valve components boiler firewall	Powder feed
FIAT	Valve stem valve seat aluminum block	Cr, C, Cr, Ni, Mo/cast Fe preplaced powder
GM	Automotive	Cast-iron systems
Rockwell	Aerospace	T-800, stellites, powder feed
Westinghouse	Turbine blades	Stellites, colmonoys preplaced beds and gravity
NRL	Proprietary	Multiple alloy, powder feed

Superficial melting of the substrate surface is required so that a fusion bond takes place. The particles need not necessarily arrive at the melt pool surface in a molten state. In fact, theoretical calculations and high-speed photography show that an average size particle hardly gets red hot while traveling through the beam (12).

Solid particles are often observed in plasma-sprayed coatings. In powder injection laser cladding, no embedded solid particles were observed in the cast structures. It has been shown theoretically that the melting time of a particle is much lower than its time of residence

TABLE 2.

Process	Interface Bond S = Solid L = Liquid Clad Subs		Dilution %	Deposition Rate 16/hr	Min. Thickness In.	Heat Spot Size In.	Appl. to Automations	Appl. to Internal L = Large only	Surface Finish
Flame Spray	L	S	1-10	1-6	1/32	1			S
Fuseweld	S/L	S	1-30						S
Oxyacet +Rod	L	L	15-25			1			
MMA	L	L	15-25	5-25	1/8	1/2			
MIG	L	L		1-6	1/8	1/2	x	L	
GTA, TIG	L	L	10-20	1-8	1/32	1/2	x	L	
Plasma TR Arc	L	L	5-25	1-15	1/16		x	L	
Plasma Spray	L	S	5-30	1-15	1/32	1/2	x	L	S
Plasma Spray	L	L	5-30				x	L	S
Saw	L	L	10-50	10-60	1/8-5/16	2	x		
Plasma + FNC	L	S/L	1-30						S
Roll bonding	S	S	0						(S)
Explosion	S	S	0		1/8			L*	(S)
Detonation	S	S	0		1/64				S
Electroplate	S	S	0		10 ⁻⁵		x	x	S
PVD	S	S	0		0			x	S
CVD	S	S	0		0			x	S
Ion Plating	S	S	0		0			x	S
5 kW Laser	S/L	L	0-90	1-10	1/64	1/100	-1/2	x	S
			Control-table			Control-table	x	x	if correct

within the superheated melt pool (10). Also, theoretical calculations show that particles may penetrate the melt pool surface only to a shallow depth before melting completely or may ricochet from the melt surface if the impact angle becomes smaller than a critical angle for ricochet.

Particles falling on the "mushy" region leave a "crater" and, as a result, the surface of the clad bead appears to be "pock-marked," Fig. 6. Normally, as much as 80% of the powder falling on the molten pool is utilized to create the clad bead. However, the overall powder utilization will be much lower if the particles falling on the area surrounding the melt pool are also accounted. Recycling of powder is possible if there is efficient shrouding.

The process parameters are listed in Table 3, categorized into three systems: laser, powder injection and substrate handling.

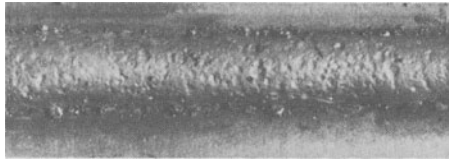


FIGURE 6. Characteristic "pock-marked" surface finish of a clad bead.

3. EVALUATION OF CLADDING RATES

From numerous experiments, Weerasinghe (10,3) was able to draw up the following equations relating the geometry of the deposit tracks to the cladding rate:

$$\begin{aligned} S &= a - bW \\ K &= \exp(-T/1.8H) \\ SH &= d \\ C &= KWS = xS \end{aligned}$$

where

$$\begin{aligned} S &= \text{cladding speed mm/s} \\ W &= \text{single-track width mm} \\ H &= \text{single-track height mm} \\ T &= \text{uniform clad thickness mm} \\ K &= \text{overlap factor defined as } (x/W) \\ x &= \text{transverse traverse mm} \\ C &= \text{cladding rate mm}^2/\text{s} \\ a, b, d &= \text{constants} \end{aligned}$$

For a laser power of 3 kW and beam diameter of 5 mm the constants are:

$$a = 57.36, \quad b = 10.81, \quad d = 5.17$$

It is seen that there is an optimum overlap factor "K" for a given clad thickness "T," since the same clad thickness can be obtained with a low "K" and a high "S" or a high "K" and a low "S." The optimum "K" is that which gives the maximum "C" and is found by differentiation of $C = f(K, T)$. Such calculations are presented in Fig. 7, showing the maximum cladding rate for a particular clad thickness.

TABLE 3. Main operating variables for laser cladding by powder injection (typical values are given in brackets).

System Variable	Method of Monitoring
LASER - cw, CO ₂	
Power (up to 3 kW)	Flowing cone calorimeter
Beam diameter (1-5 mm)	Rotating rod ((LBA) 14,15)
Mode structure	Prints, optical geometry, fluorescent screens, LBA
POWDER INJECTION	
Mass flow rate (0.04-0.35 g/s inside diameter of injector tube 3 mm)	Acoustic emission sensor on feed line
Particle velocity (1.4 m/s for conveying gas velocity of 5.8 m/s)	Rotameters, fast-action cinematography, photographic tracer technique
Particles shape and size (-100 mesh, avg. size 60 μ m)	Microscopy, sieve analysis
SUBSTRATE MOVEMENT	
<u>Traverse speed</u> 5-50 mm/s	Electronic timer
<u>Traverse index</u> (manual 0.3-2.0 mm)	Scale calibrated to 0.1 mm

* Other monitoring methods available for some aspects.

It is noted that the graphs in Fig. 7 go through the origin (0,0). However, it must be stated that there is a definite region within which satisfactory cladding is obtained. Although the graphs can be extrapolated to high power levels, they cannot be safely extended to power levels below about 1.0 kW if using a 5 mm spot. There is a low and a high speed limit, both depending on the laser power or rather the power density (i.e., power/spot area) and the powder mass flow. The high speed limit is where cladding ceases due to insufficient heat input to melt the substrate surface. The low speed limit is where the high specific energy input distorts the substrate plate to unacceptable levels and/or the process becomes uneconomical.

The cladding rates shown in Fig. 7 can be greatly enhanced by using a hemispherical reflector to recycle the reflected energy losses, Figs. 8 and 9, and shot-blasting the substrate surface, Fig. 10.

By offsetting the axis of the beam to the axis of the dome, the reflected beam could be positioned away from the main beam and so be

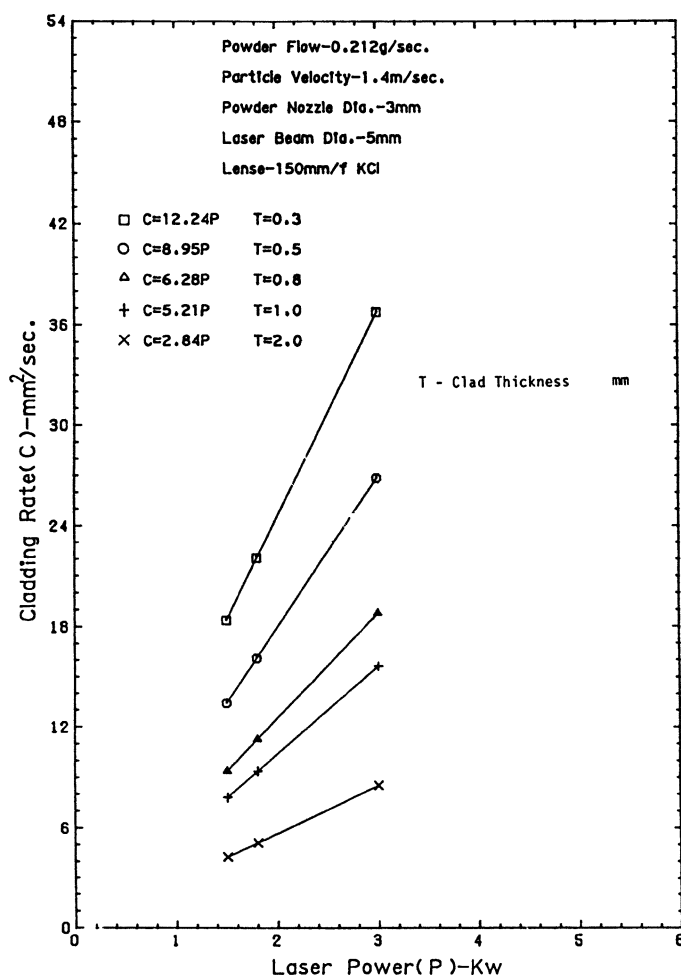


FIGURE 7. Cladding coverage rates calculated from relationship in Section 3, not experimental data.

used for either pre or post heat, Fig. 11. It also allows an experimental determination of the reflected energy by collecting the reflected radiation in a calorimeter. Thus this device, when clean, recycles some 40% of the incident beam energy.

Referring to Fig. 9, it can be seen that the advantage of using the reflecting dome is greater for thinner clad thicknesses, i.e., at higher cladding speeds. This is because at high cladding speeds, a small area is heated to high temperatures compared to the total area on which the laser beam is incident. Since reflectivity reduces at high temperatures, then at high cladding speeds with reduced temperatures, a higher proportion of the incident laser power will be reflected.

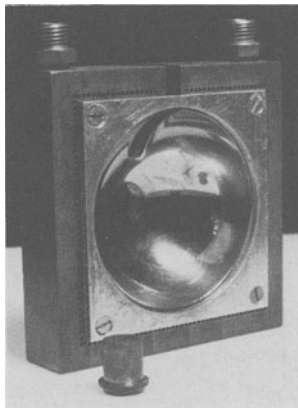


FIGURE 8. Spherical reflecting dome.

4. THREE BASIC BEAD PROFILES

Three basic single-track bead profiles emerged from the numerous section profiles which were examined, Fig. 12.

Profile "c" with an obtuse contact angle is the preferred section for low-dilution cladding. At higher powder feed rates or slower speeds, profile "a" is produced, while at lower powder feed rates and/or higher power densities, profile "b" is produced.

Multiple-track clad layers produced by overlapping of profile "c" will be of good surface finish, minimum or no porosity, and of no dilution. Profile "a" will produce multiple-track clad layers of poor surface finish, greater thickness, no dilution and heavy porosity, especially at the root in between runs. Clad layers produced by profile "b" will be of good surface finish, no porosity, high dilution and generally of lesser thickness than "c". Further, the penetration pattern shown in Fig. 12 is characteristic of a Gaussian beam where there is a peak power intensity at the center. (With a "doughnut" beam, the penetration is more pronounced at the bead edges and is generally of less severity.)

5. EFFECT OF POWDER INJECTION PARAMETERS

The extent of dilution is controlled by the injected powder mass flow or rather the powder flux (g/smm^2), Fig. 13. The optimum powder flux is that which gives the minimum dilution and maximum depositon. It is dependent on the power density (W/mm^2) and mode structure of the laser beam but is independent of the cladding speed. For a lower powder flux the dilution will increase and mass depositon decrease. For a higher powder flux, the effect is reversed.

The optimum powder mass flow was found to be directly proportional to $(P/D \times n)$ where "P" is the laser power, "D" the spot diameter, and "n" is a beam shape factor depending on the power intensity distribution.

The optimum stainless powder (~ 100 mesh size) flux was found to be 10 mg/S mm^2 for a laser power of 1800 W, spot diameter of 5 mm, and a "doughnut" intensity distribution TEM 01*. A 10% higher flux was required for a Gaussian beam due to its more central power distribution.

A 10% increase in the cladding rate was obtained when the average particle size was reduced from 77 microns to 58 microns (3).

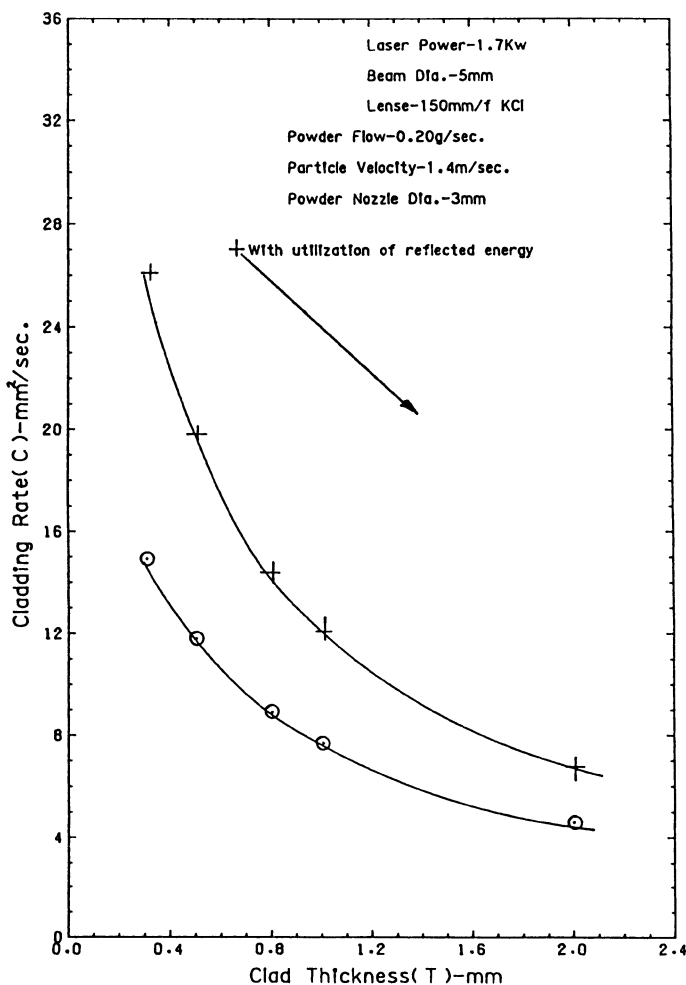


FIGURE 9. Effect of recycling the reflected energy on cladding rate.

A low particle velocity (1.4 m/s) is desirable to minimize ejection and ricochet losses from the molten pool. Since there is a minimum gas velocity required for efficient conveying (2.8 m/s), a limit is imposed. However, some amount of gas can be purged through fine holes near the injector tube exit and so reduce the particle velocity (3).

The major effect of the powder injection angle is due to the variation of the powder flux (g/mm^2) input to the molten pool. The distance from the molten pool to the injector tube has a similar effect due to divergence of the powder clad.

The powder jet is positioned in relation to the beam so that the whole of the molten pool is flooded with powder. Normally, only about

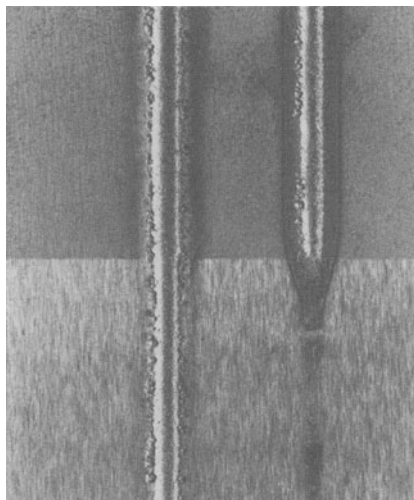


FIGURE 10. Effect of shot blasting the substrate surface. The top half of the substrate surface is shot blasted. The bottom was masked to retain the original ground finish. The track on the left was produced with the "dome" and continues on both sections, since the reflected energy is recycled.

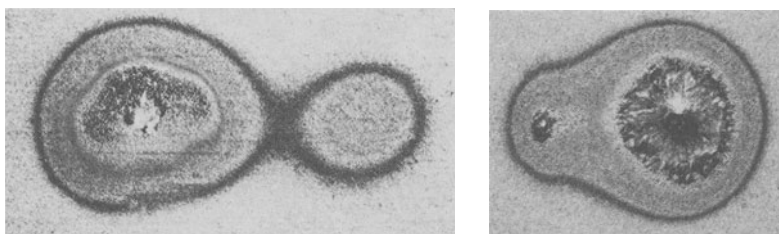


FIGURE 11. Reflected beam (right), positioned away from the main beam (left).

10% of the laser power is absorbed by the powder cloud. This was verified by theoretical calculation and by experiment (3).

In practice, an injection angle of $45\text{--}38^\circ$ (defined from the horizontal) was used with a distance to the molten pool around 10-12 mm from the injector tube end.

6. EFFECT OF LASER BEAM PARAMETERS

Power, spot diameter and mode structure are the beam parameters. Effects due to beam polarization are well known in cutting (16), namely, preferential absorption at a certain orientation of the cut leading edge. See the paper by Keilmann in Chapter 1 of this book. A similar situation

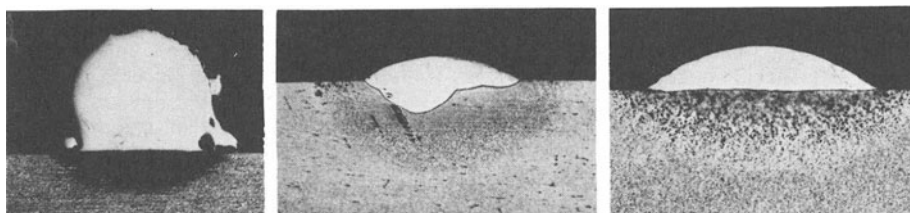


FIGURE 12. Three basic single-track bead profiles.

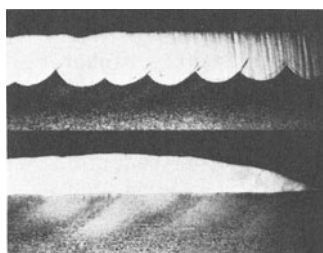


FIGURE 13. Control of dilution by powder mass flow. Powder flow 0.090 g/s top, 0.212 g/s bottom.

exists in cladding where the molten pool leading edge is inclined at an angle and also when overlapping. These polarization effects were not investigated in the present study, but are certainly not as marked as in cutting.

The spatial power intensity distribution of a laser beam is not uniform. In fact, it can be a complex distribution depending on the beam mode. Two distribution patterns commonly found in gas lasers are the Gaussian and the "doughnut," known as TEM 00 and TEM 01*, respectively.

The Gaussian beam is superior for cutting and welding applications, whereas for surface treatment the "doughnut" mode is preferred because of its more uniform heating effect. In cladding this effect is utilized to minimize dilution and obtain a desirable bead profile. Beam symmetry is also important.

An inherent advantage of using a laser as a heat source is that the source input can be localized to a small area. However, such localized heating causes rapid self-quenching and steep temperature gradients. In melting, these effects often cause solidification cracking.

In the present study a low power density, i.e., a large spot diameter of 5 mm, is used, coupled with slow speeds, to produce crack-free clad layers. Many other factors can affect this too.

7. METALLURGICAL AND PHYSICAL ASPECTS OF A LASER-CLAD AUSTENITIC STAINLESS 316 LAYER

A detailed evaluation (including corrosion properties) is the subject of a future paper. A summary is presented here in order to illustrate many aspects which may not be peculiar to stainless steel.

7.1. Surface finish

The surface finish of a clad layer produced by overlapping of single-clad beads is characterized by the "peak and valley" effect (see Fig. 4(a)). A typical "peak to valley" distance of $40\text{ }\mu\text{m}$ can be obtained with a bead of obtuse contact angle (see Fig. 12(c)) and a 60% overlap (as compared to 0.15 mm typically with weld overlay). The surface finish can be evaluated further from the amount of material which needs to be removed to obtain a clear surface (after the plate is mangled flat). A typical value per unit area is 0.6 Kg/m^2 .

7.2. Porosity

Porosity in laser-clad layers may be caused by one or a combination of the following: cavities between two overlapped beads (usually formed near the root and will be referred to as inter-run porosity), solidification cavities and/or gas evolution.

Solidification cavities occur as porosity at or near the interface. If the clad layer has a significantly higher melting point than the substrate, the solidification front may finish at the interface, thus causing shrinkage cavities (e.g., stainless steels - aluminum).

In conventional welding, porosity attributed to gas evolution by way of dissolved gases and oxidation reactions is well known, and such phenomena are also applicable in laser cladding.

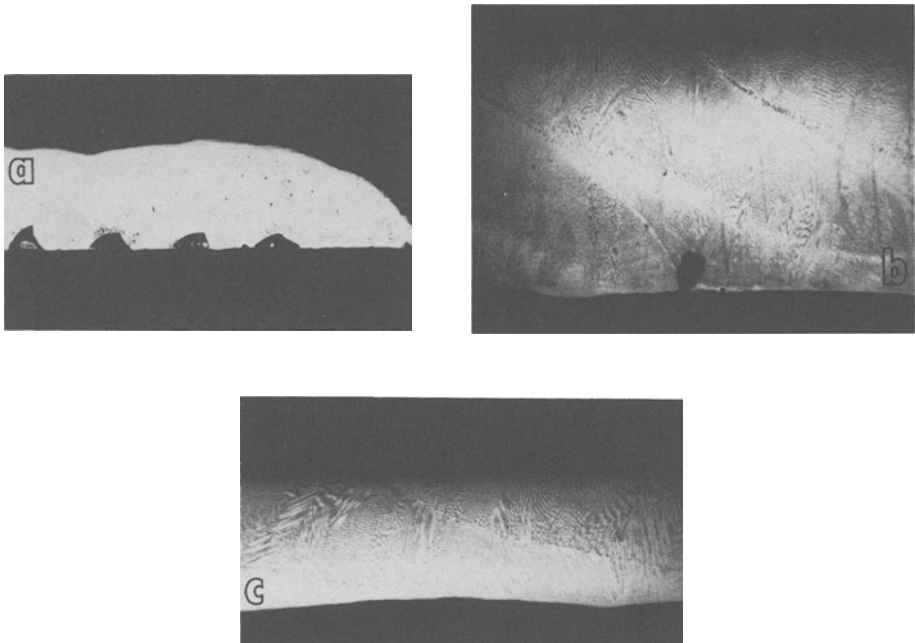


FIGURE 14. (a) Inter-run porosity, (b) location of pore in relation to interfaces shown by etching. The substrate appears totally blackened; (c) a clad layer with no porosity produced with beds of low contact angle.

In cladding stainless steel to mild steel, use of a good shrouding technique and use of dried powder limit the problem to inter-run porosity.

The formation of inter-run porosity is due to a purely "physical" effect, i.e., the contact angle of a single bead or the leading contact angle of an overlapped bead, Fig. 14(a,b,c).

In general, a bead width/height ratio of greater than five (i.e., contact angle 43°) and a percentage overlap of less than 70% will produce clad layers of no inter-run porosity.

7.3. Residual stress/plate distortion

Distortion of laser-clad plates is very small, typically a 5 m radius for a 1.4 mm clad on a 12.5 mm plate. There is minimal thermal penetration of the substrate, the heat-affected zone being of the order 1-2 mm.

Surface residual stresses were measured using the X-ray diffraction method. High tensile stresses of the order 285MPa were found on the clad surfaces. Using a pre-tensioning technique, it was possible to reduce the residual stress dramatically to compressive 8MPa (3).

7.4. Mechanical properties

Satisfactory results were obtained from tensile, bend and shear tests carried out in accordance to ASTM 264, Fig. 15(a,b).

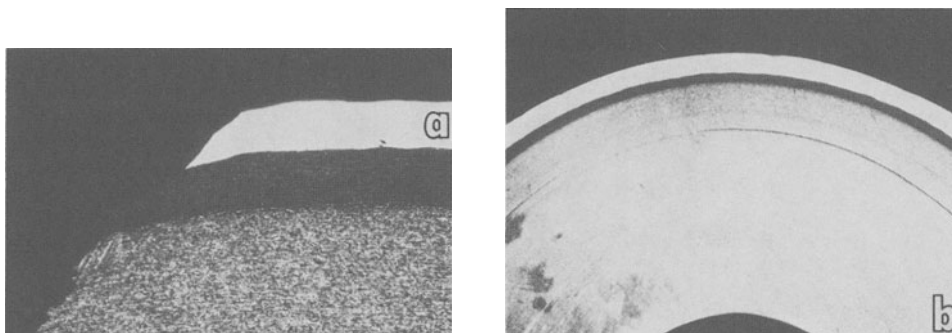


FIGURE 15. (a) Section of fracture surface of tensile specimen showing no delamination of the clad layer. Clad thickness 1.5 mm. (b) Bend test specimen - 12.5 mm thick mild steel clad with 1.5 mm thick stainless.

7.5. Microstructure

The dendritic microstructure of the laser-clad stainless 316L layer was observed to be basically similar to that of a conventional weld bead or a submerged arc strip clad, i.e., austenitic matrix with residual delta ferrite. The dendrite size is much finer due to the higher cooling rate, Fig. 16(a,b).

7.6. Cracking

In hardfacing, cracking is related to the hardness of the clad layer and can be eliminated by substrate pre-heat, Fig. 17. In austenitic stainless steels, cracking is known to take place at high temperatures (1200°C), and as such, preheating has proved to be ineffective (17).

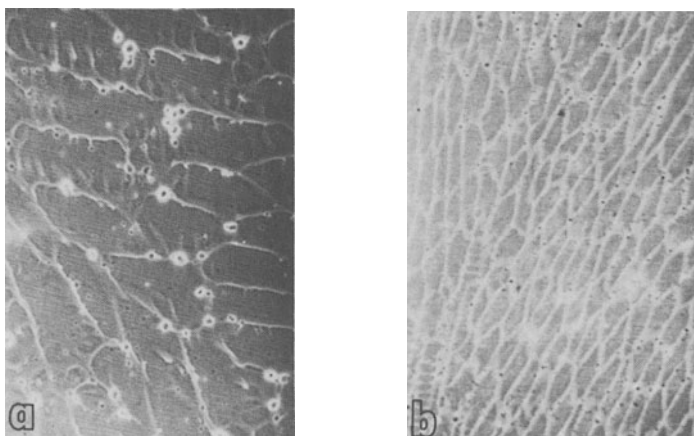


FIGURE 16. Effect of cooling rate on dendrite size - SEM micrographs. (a) cladding speed 7 mm/sec, 92 W/mm², dendrite size 6 μ m. (b) cladding speed 40 mm/sec, 573 W/mm², dendrite size 2 μ m.

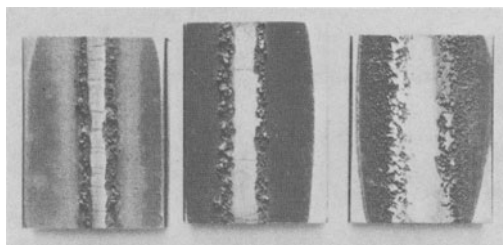


FIGURE 17. Progressive elimination of cracking by preheating the substrate. Clad-iron boron (1000 HV) substrate - mild steel.

Interdendritic cracking was observed in stainless clad layers produced at high cladding speeds (>20 mm/s) with high power densities (>366 W/mm²). Crack-free clad layers were produced at lower power densities coupled with slower speeds.

7.7. Chemical composition/homogeneity/dilution

Figure 18(a,b) illustrates the distribution of alloying elements in a 316 stainless clad layer and in the interface region, showing no macro-segregation and negligible dilution.

One may define the dilution as the compositional difference between the injected powder and the clad layer. Very low dilution was observed near the clad surface, with an overall dilution of about 5% typical. Also, Fig. 19 shows that even with high penetration, dilution is mainly confined to the interfacial region, indicating perhaps the "calmness" of the process. However, work from Takeda (6) using copper markers to illustrate the flow within the clad track suggests that there is considerable mixing turbulence.

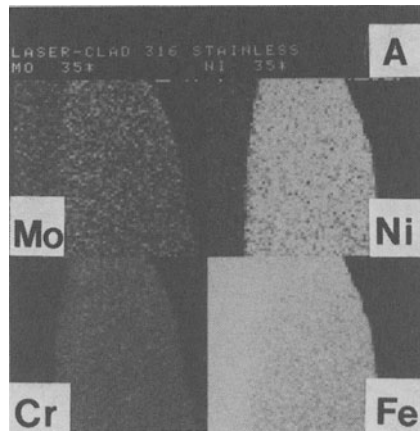


FIGURE 18. (a) X-ray digimap of alloying elements in a stainless 316 clad layer.



FIGURE 18. (b) line scan of chromium across the clad/substrate interface.

8. OTHER CLAD/SUBSTRATE COMBINATIONS

In addition to stainless/mild steel, the following clad/substrate combinations were produced using the laser:

Note: Stellite SF6 is a cobalt-based hardfacing alloy	(a) Nickel/mild steel	
	(b) Bronze/mild steel	Some porosity but
	(c) Stellite SF6/brass	good bond strength
	(d) Chromium/titanium	
	(e) Stainless/aluminum	Cracking plus
	(f) Iron boron/mild steel	delamination in "e"
	(g) Stellite SF6/mild steel	
	(h) Mild steel/stainless	

9. CONCLUSIONS

The process may be evaluated in terms of economic, engineering and quality assurance aspects.

Engineering aspects present less of a problem since they are mostly similar to other laser-processing applications which have already found industrial acceptance; except perhaps aspects of powder injection, which have now been developed to a reliable level.

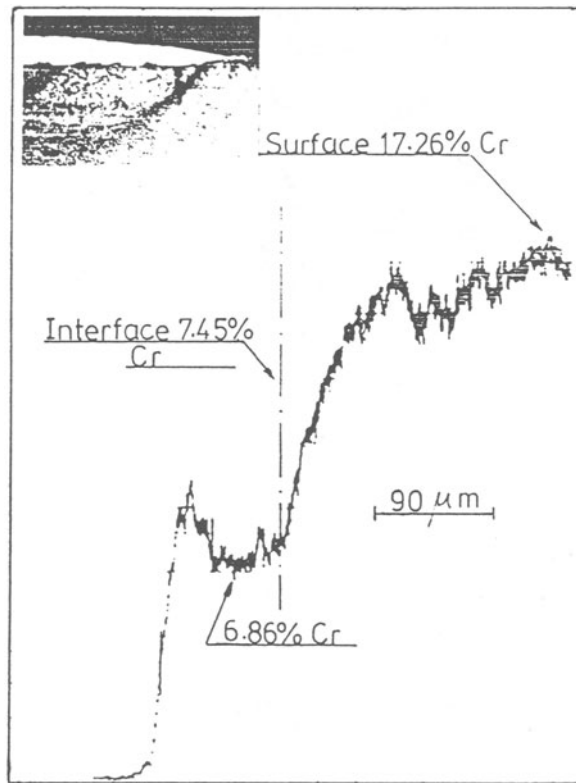


FIGURE 19. Crystal spectrometer scan of chromium across the thickness of a clad layer with high penetration.

From a metallurgical/physical evaluation of a representative clad/substrate combination of austenitic stainless steel and mild steel, there is conclusive evidence that clad layers of acceptable quality can be produced using the laser. Similar data is being found for other systems.

From the economic assessment there is no doubt that laser cladding is best suited for treatment of small confined areas, such as valve seatings, turbine blade edges, wear surfaces of tools, etc. Deposition of thin coatings of expensive materials is also a good application. Laser cladding of large areas may be cost effective if adaptive automation of the process can be achieved, whereby the process will automatically correct itself for heating effects on the substrate.

REFERENCES

1. J. Powell, Proc. Conf. on "Surface Engineering with Lasers," London, May 1985, Paper 17, publ. Metal Society, London.
2. V. M. Weerasinghe and W. M. Steen, "Laser Cladding with Pneumatic Powder Feed, Proc. 4th Int. Conf on Laser Processing, Los Angeles, Jan. 1983.
3. V. M. Weerasinghe, Ph.D. Thesis, London University, 1985.
4. S. Dallaire and P. Cielo, "Pulsed Laser Treatment of Plasma Sprayed Coatings," Met. Trans B V 13B N E Sept. 1982, pp. 479-483.
5. H. Bhat, R. A. Zatorski, H. Herman and R. J. Coyle, "Laser Treatment of Plasma Sprayed Coatings, Proc. 10th Int. Conf. on Thermal Spraying, Essen, W. Germany, pp. 2-6, May 1983, Publ. Deutscher Verlag für Schweisstechnik GmbH Dusseldorf, W. Germany, 1983.
6. T. Takeda, W. M. Steen, and D. R. F. West, "in situ Clad Alloy Formation by Laser Cladding," Proc. LIM 2, Birmingham, UK, March 1985, publ. by IFS Publications Ltd., Bedford UK.
7. J. Powell and W. M. Steen, "Vibrolaser Cladding," Laser in Metallurgy, edited by K. Mukherjee and J. Mazumder, publ. Met. Soc. of AIME, Warrendale, PA, USA, pp.93-104.
8. M. MacIntyre, "Laser Hardfacing of RB 211 Turbine Blade Shroud Interlocks," Proc. 2nd Int. Conf. on Applications of Lasers in Material Processing, Jan. 1983, Los Angeles, USA.
9. M. Eboo and A. E. Lindemanis, "Advances in Laser Cladding Technology," LIA Conf., Los Angeles, March 1985.
10. W. M. Steen, Laser Cladding," Metals and Materials Tech., to be published.
11. UK Patent No. app. 84 25716, Quantum Laser Corp., USA.
12. J. Powell, Ph.D. Thesis, Univ. of London, 1983.
13. V. M. Weerasinghe and W. M. Steen, Computer Simulation Model for Laser Cladding by Powder Injection, Conf. Proc. ASME, Boston, Nov. 1983.
14. G. C. Lim and W. M. Steen, "Measurement of Temporal and Spatial Power Distribution of a High-Powered CO₂ Laser Beam," Optical and Laser Tech., June 1982.
15. A. L. L. Brochure, Hans Gressel weg. Munchen - 8000, W. Germany, 1982.
16. J. N. Kamalu, Ph.D. Thesis, Univ. of London, 1981.
17. J. Alexander, Ph.D. Thesis, University of London, 1982.
18. R. Castro and J. J. Cadenet, Welding Metallurgy of Stainless and Heat-Resisting Steels, Cambridge Univ. Press, 1974.